Experiments in Fluids 12, 200–208 (1992)

Experiments in Fluids

Blade manipulators in turbulent channel flow

B. Vasudevan, A. Prabhu and **R. Narasimha** *

Department of Aerospace Engineering, Indian Institute of Science, Bangalore 560 012, India

Abstract. We report here the results of a series of careful experiments in turbulent channel flow, using various configurations of blade manipulators suggested as optimal in earlier boundary layer studies. The mass flow in the channel could be held constant to better than 0.1%, and the uncertainties in pressure loss measurements were less than 0.1 mm of water; it was therefore possible to make accurate estimates of the global effects of blade manipulation of a kind that are difficult in boundary layer flows. The flow was fully developed at the station where the blades were mounted, and always relaxed to the same state sufficiently far downstream. It is found that, for a given mass flow, the pressure drop to any station downstream is always higher in the manipulated than in the unmanipulated flow, demonstrating that none of the blade manipulators tried reduces net duct losses. However the net increase in duct losses is less than the drag of the blade even in laminar flow, showing that there is a net reduction in the total skin friction drag experienced by the duct, but this relief is only about 20% of the manipulator drag at most.

List of symbols

A, A'	log law constants
c	chord length of manipulator
D	drag of the manipulator
dp/dx	pressure gradient in the channel
h	half height of the channel
H	height of the channel (2h)
K	log law constant
L	length of the channel
L.E.	leading edge of the manipulator
P	static pressure
P_x	static pressure at a location x on the channel
P_{xm}	static pressure at the location x in the presence of manipulator
p_{ref}	static pressure at any reference location x upstream of the manipulator
Re	Reynolds number
t	thickness of the manipulator
T.E.	trailing edge of the manipulator
u	velocity in the channel
U_*	friction velocity
$\bar{U}$	average velocity in the channel
u_c	centre-line velocity in the channel
U_+	U/U_*
u_m	velocities in the channel downstream of the manipulators
u_{ref}	velocities in the channel at reference location upstream of the manipulators
w	Coles's wake function
W	width of channel

1 Introduction

Studies during the past decade have suggested the possibility that active and passive devices interfering with the ordered structure of a turbulent boundary layer may lead to reduced drag. Extensive surveys by Bushnell (1983), Nagib (1983) and Wilkinson et al. (1987) summarize the status of research on these devices, among which blade manipulators (also variously called large-eddy breakup devices (LEBUS) and ribbons) have attracted considerable attention. Early work by Yajnik and Acharya (1977) with honeycombs and screens in a turbulent boundary layer suggested a reduction of upto 50% in skin friction, over part of the surface, but the drag of the device itself was equivalent to a 500% increase in the surface drag over the same distance. Blade manipulators have been extensively investigated by Corke et al. (1979), Hefner et al. (1980), Bertelrud et al. (1982), Anders et al. (1985), Plesniak and Nagib (1985), Poddar and Van Atta (1985), Coustols and Cousteix (1986) and Mumford and Savill (1988). Many of these studies have suggested reduction in net drag in the range of 4 to 20%.

Narasimha and Sreenivasan (1985) have reviewed these studies in detail, and point out that what they call the "wake effect", arising from the insertion of any object in the boundary layer, will by itself always decrease the friction drag, and indeed (when resulting in flow separation) could even produce a friction thrust! This of course is of no interest in itself, but the possibility remains that what they call the "blade effect", which suppresses normal velocity over the blade and also generates vortices responsible for any lift that may act on the blade, could favourably modify the turbulent structure. A small reduction on net drag was not ruled out in a certain domain of blade chord and wake thickness.

However, the evidence presented by various authors suggesting large net reductions in drag cannot be regarded as

* Also National Aeronautical Laboratory, Bangalore 560 017, India

conclusive because of (a) the great difficulty of making accurate measurements of total drag on a flat plate, and (b) uncertainties in the measurement of skin friction and the evaluation of net drag by indirect methods such as either momentum balance or wall similarity techniques. These uncertainties arise from the lack of similarity in the manipulated wall layer (making some conventional skin-friction instruments relying on similarity less trust-worthy: see Takagi (1983 a, b)) and from possible lack of two-dimensionality in the flow, making interpretation of momentum thickness data difficult.

Experiments in a duct are clearly less vulnerable to such uncertainties. The pressure drop in the duct can be very accurately measured for a given mass flow, with and without these devices, and so can provide unambiguous data about net drag. Furthermore, the large eddy structure in channel flow is virtually the same as in a boundary layer (Luchik and Tiederman 1987), so conclusions from experiments conducted in a channel should have wider significance.

Preliminary results of measurements carried out by the authors in a channel were earlier presented at a IUTAM conference (Prabhu et al. 1987), and showed no net drag reduction for any of the blade configurations studied. Since then the apparatus has been considerably improved, in order to provide cleaner flow and greater accuracy in measurement. Meanwhile Sahlin et al. (1988) have reported no drag reduction in flat-plate studies. Manipulated pipe flows have also been investigated (Pollard et al. 1989, 1990), but the channel has the advantage of not requiring the additional struts necessary for supporting the manipulator rings used in pipes. The present studies are to the best of our knowledge the only ones where the relaxation of the flow to equilibrium after manipulation is complete. The fact that such relaxation occurs at all is of fundamental importance in the light of the paradox in manipulated boundary layers discussed by Narasimha and Sreenivasan (1988).

Because the experiments are delicate in some sense (drag differences under discussion are of the order of 10 N, or a few percent of the total drag), it is essential that the flow quality should be good. We therefore devote some space to describing how this was achieved in the present experiments.

2 Experimental setup

2.1 Channel

The channel used in the present studies is shown schematically in Fig. 1, the overall dimensions being 50.8 mm × 545 mm × 7315 mm. The top and bottom surfaces of the channel are made by assembling three sections of plywood (each 8 feet (2.44 m) long and 12 mm thick) onto 1.6 mm thick aluminium plates and gluing them together with fevicol SR 998. The side walls of the channel are made of standard 12 feet (3.66 m) long aluminium channels (50.8 mm × 50.8 mm × 6 mm). Ten precisely machined tem-

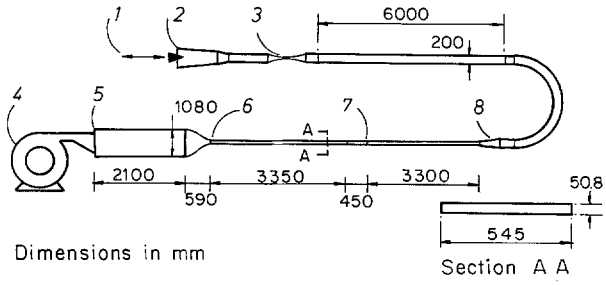

Fig. 1. Schematic layout of channel facility. *1* Speed control, *2* Diffuser, *3* Venturi, *4* Blower, *5* Settling chamber, *6* Boundary Layer Trip, *7* Manipulator section, *8* Transition section

plates are used to keep the width of the channel constant while assembling the channel. Fifty 3-inch screw jacks along the channel enable accurate levelling of the facility on its supporting structure (to an accuracy of better than 0.5 mm between the ends of the channel). Three coats of clear polyurethane paint cover all the four inner walls of the channel. The top and bottom walls are stiffened with 25 × 25 × 5 mm mild steel sections in both axial and transverse directions, the longer sections being joined by 100 × 25 × 5 mm mild steel channels. The flow is driven by a 10 HP blower, isolated from the channel by a flexible bellow. A fabric filter of mesh size 10 μm is provided in the settling chamber. The boundary layer at the channel inlet is tripped using coarse carborundum grit on both top and bottom walls. A fetch of seventy five channel heights ensures fully developed channel flow at the manipulator station. The channel is provided with 201 static pressure taps along the axial direction (at an interval of 25 mm along the centre-line downstream of the manipulators), and 102 taps in the transverse direction.

At the end of the channel, a transition piece smoothly converts the rectangular section to a 200 mm dia circular section, which turns back on itself through a large-radius 180° bend and continues for 6.0 m towards a 110 mm dia. Venturi, made strictly in accordance with BS 1042, for measuring the mass flow. Downstream of the Venturi is a centre body in the shape of a sharpnosed square pyramid whose movement along the axis provides control over the mass flow in the channel.

2.2 Instrumentation

Figure 2 shows a schematic of the instrumentation set up. Pressure drop across the Venturi (≃ 150 mm alcohol) is measured with a projection manometer of resolution 0.1 mm, which permits control of mass flow in the channel to an accuracy of better than 0.1%. Static pressures along the channel walls are measured using a capacitance type differential electronic manometer with a range of 0 to 20 mm H_2O, an accuracy of 0.5% and a resolution of 0.01 mm H_2O. This manometer is provided with an auto zero control unit. A 48-port D-type scanivalve with a controller, and a PC/AT with a 16-channel analog-to-digital card of 15 μs sampling

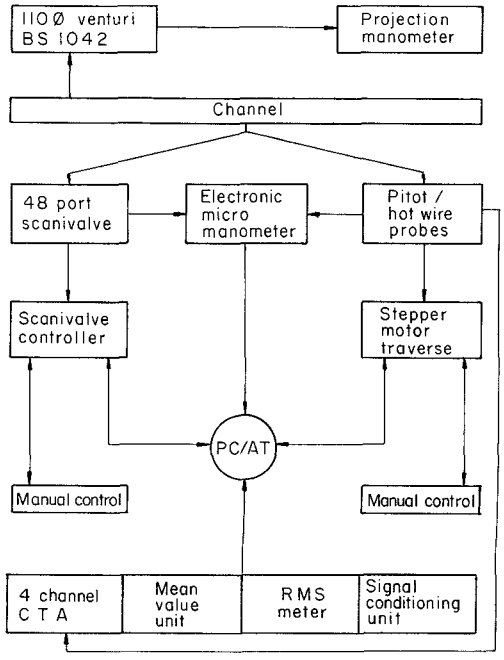

Fig. 2. Channel instrumentation

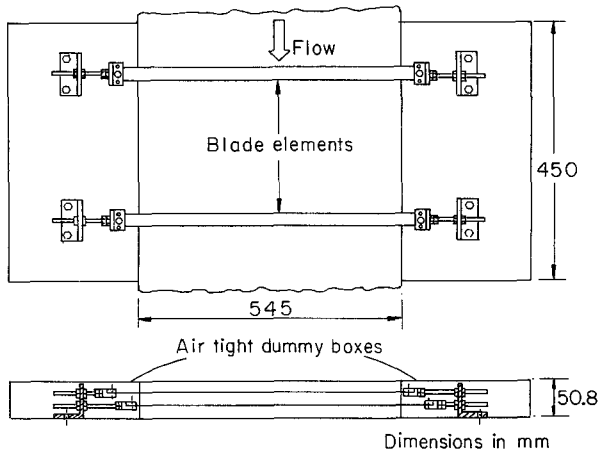

Fig. 3. Sketch of the blade manipulator section

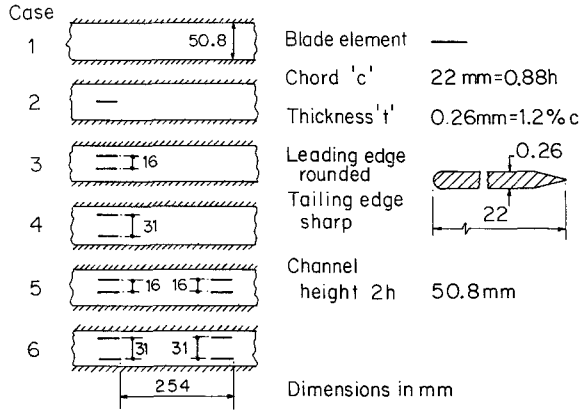

Fig. 4. Different blade element configurations

time, permit acquisition of channel pressure data at 48 locations in less than a minute. At each port, an average of about 1,000 samples was taken. The channel is also provided with a stepper-motor traverse (1-axis) with a spatial resolution of 5 μm. Circular tubes of 0.2 mm inside diameter and 0.4 mm outside diameter, as well as rectangular probes 0.6 mm × 0.25 mm (outer dimensions) were used to measure velocity profiles. A 4-channel constant-temperature hot wire anemometer, with a mean value unit, an RMS meter and associated signal conditioning units, is also connected to the PC/AT.

2.3 Manipulators

The manipulators were made by processing thin spring steel strips of high strength, bought off the shelf. The blades made from these strips for the present investigations had a thickness of 0.26 ± 0.005 mm and a chord of 22 ± 0.05 mm, with a rounded leading edge and sharp trailing edge. Figure 3 shows the blade and details of the holder with the arrangement devised for applying tension to the manipulators. A leak-proof dummy box mounted at the manipulator section on either side of the channel serves the function of locating and holding the manipulators. The bottom wall of each box is a milled aluminium plate (12.7 mm thick) level with the channel bottom wall; the top-plate is made of 12 mm plexiglass. Good O-ring seals ensure that the boxes are air-tight. At the locations where the manipulators pass through the channel side walls, specially milled grooves formed in spacer plates were attached to the side walls. These spacer plates were milled to match with the side walls of the channel. The blades were mounted horizontally (incidence zero to within $\pm 0.2°$), the specified height being obtained with the help of ground "spacer blocks" specially made for each particular height.

Figure 4 displays the various blade manipulator configurations studied, which include a single blade at the centre of the channel (case 2), stack of two blades one on either side of the channel, at two different distances from the walls (cases 3 and 4), and tandem stacks also at two different heights from the walls (cases 5 and 6). Case 1 corresponds to free channel flow. The stacked elements were at 0.68 h from the walls in cases 3 and 5 and at 0.38 h in cases 4 and 6. In the tandem configuration, the distance between the tandem blades was 254 mm corresponding to 10 half channel heights. These configurations correspond to the optimal as reported in boundary layer studies by various investigators (see Mumford and Savill (1988), Plesniak and Nagib (1985), Hefner et al. (1983), Bertelrud et al. (1982) and Anders and Watson (1985)).

3 Results and discussion

All experiments were carried out at a Reynolds number of 29,000 based on the half-height h of the channel and the centre-line velocity (u_c) of 20.4 m/s upstream of the manipulators (or 23,500 based on average velocity in the channel). The manipulator Reynolds number based on the chord and local velocity was in the range 25,500 to 27,700. This Reynolds number is sufficiently low to encourage a laminar boundary layer on the manipulators. However, it should be noted that the manipulator is embedded in a turbulent outer flow field. Careful studies carried out by Govindaraju and Chambers (1987) indicate that the drag of these devices corresponds to laminar skin friction drag computed at the chord Reynolds number provided the angle of attack is maintained close to zero. The mass flow, at nearly 0.50 kg/s, corresponds to a differential pressure of about 150 mm alcohol across the Venturi; this pressure drop could be kept constant to 0.1 mm, and the corresponding mass flow to within ±0.07%.

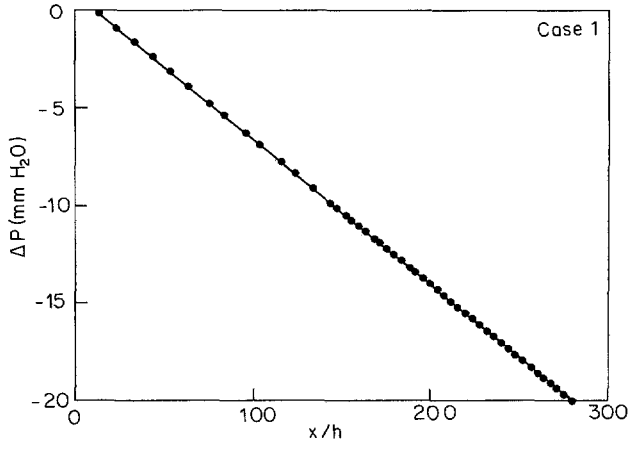

Fig. 5. Pressure drop along the length in the free channel

3.1 Flow quality in the free channel

Figure 5 shows a typical pressure distribution along the channel, and demonstrates how accurately linear the distribution is. The standard deviation of the departures from the linear fit, for any given set of measurements, was found to be lower than the stated accuracy of measurements. The repeatability of the pressure distribution in the channel indicates that the quality of flow is excellent.

The wall stress τ_w was computed from the pressure drop to be 0.760 Pa, which corresponds to a friction velocity U_* of 0.825 m/s. The friction coefficient from the present experiment is indicated for comparison in Fig. 6, which is a summary of the data for two-dimensional rectangular duct flows compiled by Dean (1978) in his comprehensive survey. The present result is seen to agree very well with the law recommended by Dean.

Figure 7 shows the unmanipulated mean velocity profile at the manipulator station. The friction velocity obtained from the pressure gradient was used for forming the inner variables used in the figure. The profile clearly shows the logarithmic variation in the inertial sublayer and the small departure therefrom at the centre of the channel, and is well represented by the Coles universal velocity distribution

$$U_+ = \frac{1}{K}[\ln y_+ + A] + \frac{\pi}{K} w\ (y/h)$$

where $w\ (y/h)$ is the wake function, π is the wake parameter, and K and A are log law constants. The values obtained in the present experiment, namely $K = 0.401$, $A = 2.30$, $\pi = 0.135$ and $A' = A + 2\pi = 2.57$, are indicated in the inset of Fig. 7 which is a summary of the results compiled by Dean, and are clearly in agreement with his proposals. The same figure also shows the mean velocity profile at a distance 40 h downstream of the blade manipulators. The coincidence of this profile with that in unmanipulated flow indicates that the manipulated flow relaxes back to fully-developed free-channel flow sufficiently far downstream.

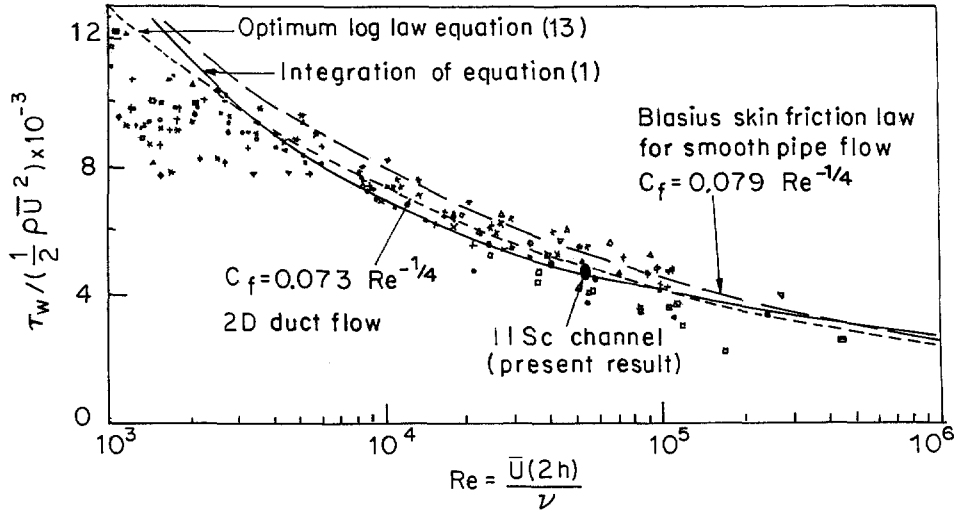

Fig. 6. Wall shear stress dependence on Reynolds number for turbulent channel flows taken from Dean (1978). IISc channel data is also shown

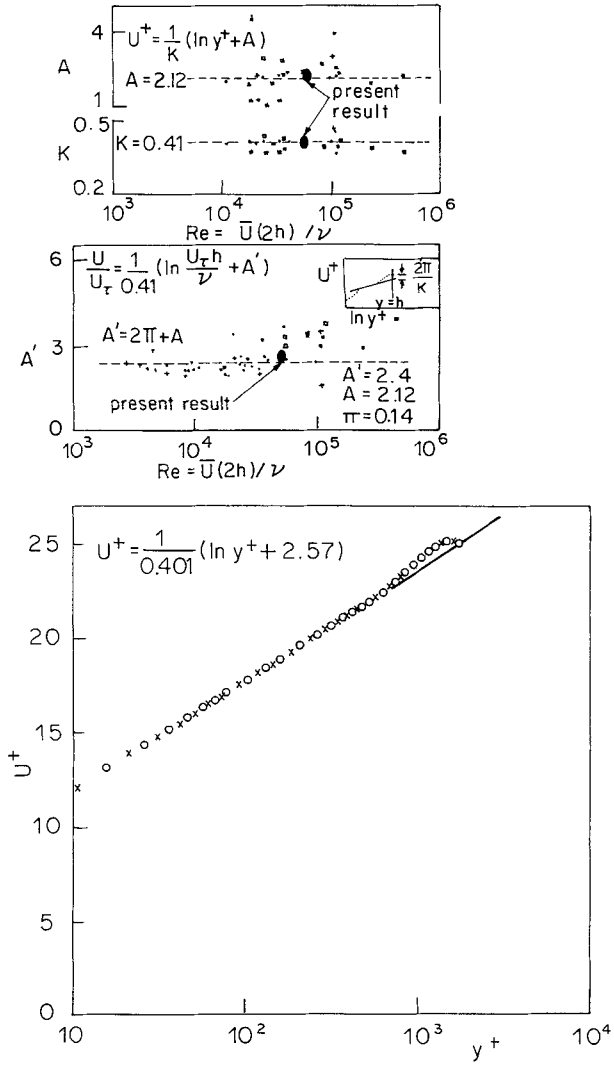

Fig. 7. Mean velocity profile in wall variables in the fully developed region of the channel. o Unmanipulated case (profile measured at the manipulator station). × Case 3 at forty channel heights downstream of the manipulator location. Top: summary of log law constants reported by Dean (1978). IISc data are also shown

Figure 8 shows that the velocity profiles at three spanwise locations (at a distance 6 h downstream of the trailing edge of the manipulators, case 3) agree among themselves very well, indicating good two-dimensionality. The inset shows the spanwise variation of pressure at two stations, respectively upstream and downstream of the manipulators, again indicating good two-dimensionality.

These measurements show that the basic flow quality can be considered to be good, enabling accurate measurement and reliable interpretation of flow changes due to manipulation.

3.2 Effect of manipulators

The blade manipulators are located at a station 73 h from the entry to the channel, where as indicated earlier the flow is

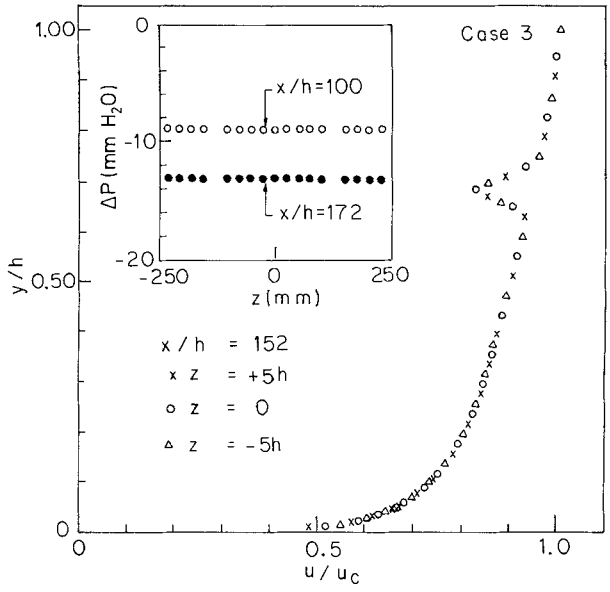

Fig. 8. Two-dimensionality of the channel flow; mean velocity profiles at 3 spanwise locations at a distance of 6 h from the manipulator trailing edge. Inset shows spanwise variation of wall static pressures at two axial locations (one upstream and another downstream of the blade elements)

already developed. The pressure drop in the manipulated flow was found to be sensitive to any vibration of the blade elements. To suppress such vibration, the blade elements were tensioned using the fixtures at the ends shown in Fig. 3 and observing the motion of sand particles sprinkled on the blades. It was found that the pressure drop behind the blades decreased in magnitude progressively as the blades were tensioned, and settled down to a constant value when the tension was sufficiently high and the vibrations ceased.

Figure 9 shows the measured pressure distributions along the channel for the different blade manipulator configurations. The distance along the channel is normalised with respect to the half-height of the channel. Manipulator positions are also indicated in the figure. For comparison, the pressure distribution in a free channel is also shown (bold line) in each case. It is seen that in none of the cases is the pressure drop with the manipulators less than that in the free channel. The increased pressure drop just behind the manipulators seems to reflect the manipulator drag, which is lowest in case 2 and highest in case 5. Case 6 has lower drag than case 5 since the local velocity at the position of the blades is lower. Similarly case 4 has lower drag than case 3. Far downstream of the manipulators the pressure distribution is seen to relax back to the same constant gradient as in free channel flow. However, the total pressure drop to any station from an upstream reference point is in no case lower and in general higher than in free channel flow.

Figure 10 shows the variations of the pressure drop between the beginning of the channel $x = x_0$ and the current location normalised by the pressure drop in the same length in the unmanipulated flow. The two peaks in cases 5 and 6

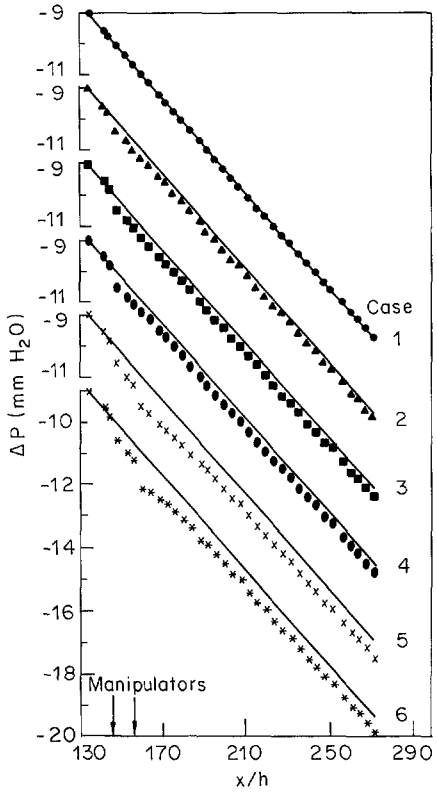

Fig. 9. Pressure drop variations along the channel for different blade element configurations. Case 1 corresponds to the free channel. All bold lines correspond to unmanipulated flow

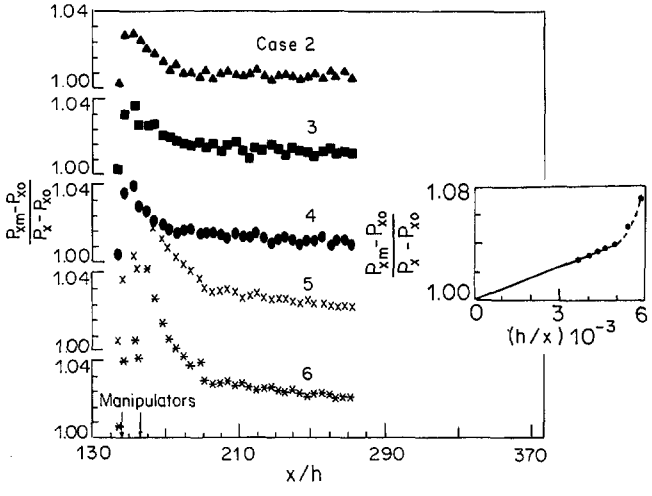

Fig. 10. Variation of pressure drop normalised with value in unmanipulated flow

are due to the tandem plates. It is again seen that the pressure drop in the manipulated flow is in general higher even at $x/h=270$. For large distances the normalised pressure in figure 10 should tend to 1 as x tends to infinity. For case 5, the observed inverse variation with x for large x shows this clearly in the inset of Fig. 10.

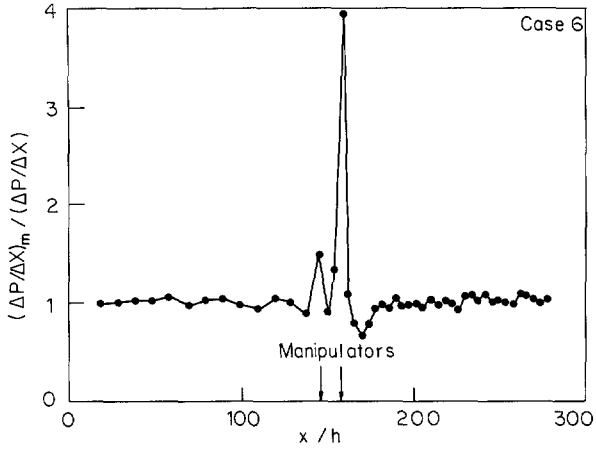

Fig. 11. Normalised pressure gradient variations along the channel for case 6

Figure 11 shows the variation of the pressure gradient along the channel (normalised with that in unmanipulated flow) for case 6. The gradient values are computed by using the pressure difference between adjacent taps and plotting the value so derived at the midpoint between taps. Since such pressure differences are very small (of the order of 0.3 mm of water) the derived gradients show appreciable scatter. However, the gradient is clearly centred around unity both upstream and beyond about 50 h downstream of the manipulators, and attains a minimum (65%) at about 14 h from the manipulator trailing edge. Such minima were found in all the cases studied, but ranged in value from 65% to 93%; they reflect a reduction in the local skin friction due to manipulation, but a direct estimate of the reduction cannot be derived without taking into account the departure of the velocity profiles behind the manipulators from those in fully developed flow because of the manipulator wake.

Figure 12 gives the normalised velocity profiles across half the channel behind manipulators for cases 3–6. The effect of the wake seems to persist upto about 40h downstream of the manipulators, but thereafter the flow has relaxed to the fully developed profile of the unmanipulated case. The average velocity across the channel (computed as $\bar{U}=1/h\int_0^h u\,dy$) for these profiles is constant to within 0.1%, which is as good as can be expected with the mass flow being held constant to the same accuracy. This constraint on U implies that the centre-line velocity varies along the channel in the developing region; it is a maximum 5 h downstream of the manipulators, relaxing back to the uniform channel value at about 40 h (Fig. 13). Just behind the manipulators, the jump in centre-line velocity is due to compensation of the mass defect in the wake. However, the increase in centre-line velocity further downstream seems to reflect a reduction of velocities near the wall accompanying a lower skin friction. All these profiles do indicate clearly a log layer near the wall. It is tempting to compute the shear stress on the channel wall using Clauser charts (with log law constants taken the same

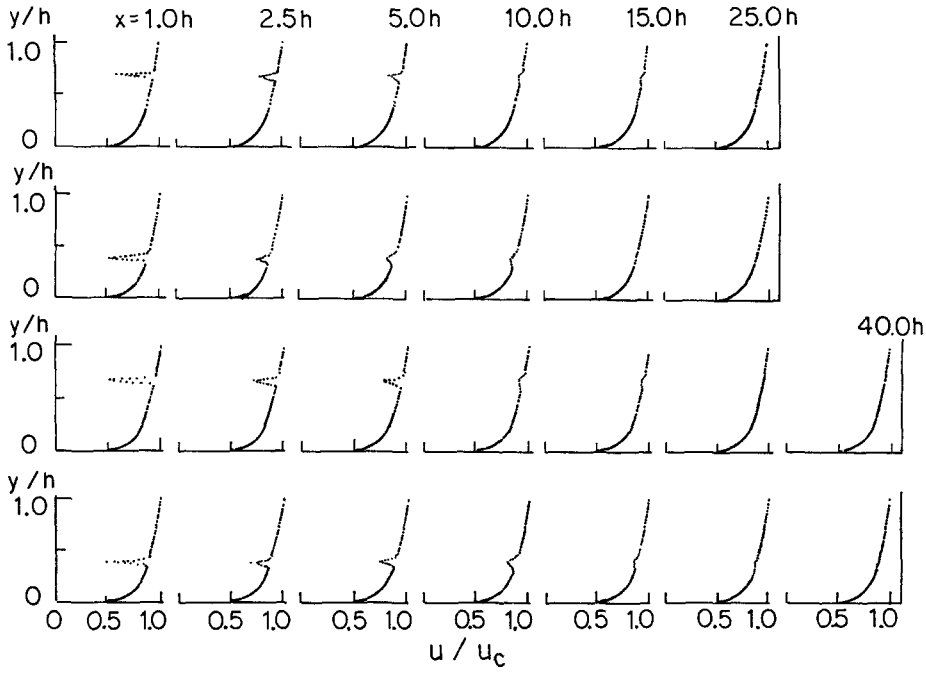

Fig. 12. Mean velocity profiles for different blade element configurations at various donwstream locations (1 h to 40 h from the manipulator trailing edge). Cases 3 to 6 from the top

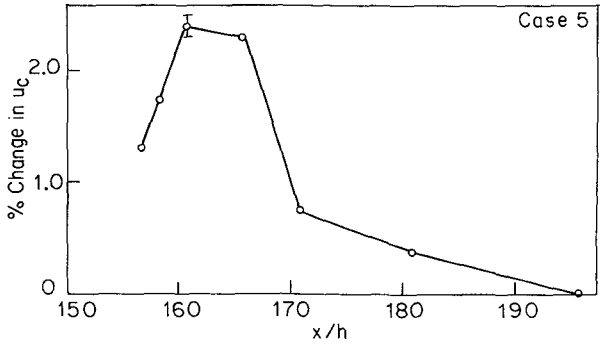

Fig. 13. Changes in centre-line velocity distributions downstream of the manipulator (case 5)

as in the free channel). If this is caried out, the reduction in the skin friction coefficient for case 5 is a maximum of about 14% and occurs around 5 h from the manipulator trailing edge; the wall stress relaxes back to the free channel value at 40 h. It was also observed that the location of the maximum centre-line velocity corresponded with that of the minimum wall stress so derived. However, the estimation of skin friction reduction based on fixed log law constants in the manipulated region may not be valid (see Truong et al. 1984, Takagi 1983 a, b, Acharya and Escudier 1983 and Poll and Watson 1984). In order to see more clearly the effect of the blade manipulators on the velocity profile development, it is useful to consider the momentum balance along the channel.

3.3 Momentum balance

Assuming that the flow is two-dimensional and that the static pressure is constant across the flow, the momentum equation integrated over the cross section of the channel yields the relation

$$-\tau_w = h(\mathrm{d}p/\mathrm{d}x) + \varrho \frac{\mathrm{d}}{\mathrm{d}x}\left[\int_0^h u^2 \,\mathrm{d}y\right]. \tag{1}$$

Where the flow is fully developed, e.g. just upstream or sufficiently far downstream of the manipulator, the second term on the right side of (1) vanishes, and the familiar relation between pressure gradient and skin friction is recovered. Where, however, the velocity profile is changing, e.g. just behind the manipulators, there will in general be a contribution from the integral in (1) to the momentum balance. Elsewhere however the term can be of either sign. The introduction of the manipulator redistributes the mean velocity in such a way that, because of the mass flow constraint, the integral in Eq. (1) is generally higher. To consider this question further without having to perform the numerical differentiations contained in (1), we integrate in x from a reference station x_{ref}:

$$-\int_{x_{\mathrm{ref}}}^{x} \tau_{wm}\,\mathrm{d}x - \int \tau_w\,(\mathrm{blade})\,\mathrm{d}x$$
$$= h(P_{xm} - P_{\mathrm{ref}}) + \varrho \int_0^h (u_m^2(x) - u_{\mathrm{ref}})\,\mathrm{d}y \tag{2}$$

The first integral on the left is the contribution from the channel walls, and the second from the manipulator. Suffi-

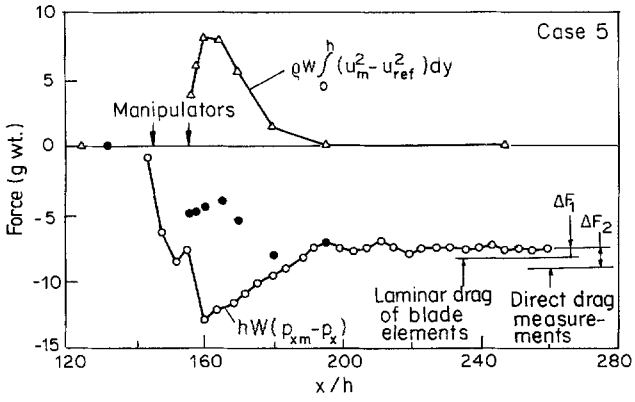

Fig. 14. Force balance in the channel for case 5. Two estimates are shown for the manipulator drag, one based on laminar flow theory and the other taken from the measurements of Govindaraju and Chambers (1987); the corresponding "relief" due to reduction in channel friction drag are shown as ΔF_1 and ΔF_2 respectively. $W(=545$ mm) is the width of the channel

ciently far downstream the second terms, respectively on the left and right of (2), are small compared to the first terms; so it is convenient for analysis to subtract from Eq. (2) a similar equation for the free channel. We then get

$$-\int_{x_{ref}}^{x}(\tau_{wm}-\tau_w)dx - D_m = h(P_{xm}-P_x)+\varrho\int(u_m^2-u_{ref}^2)\,dy\,. \quad (3)$$

I II III IV

In the above, suffix m denotes the manipulated flow, and D_m the friction drag of the manipulator (the pressure drag being assumed small, as it must be if manipulation is to work at all). Figure 14 shows the contributions from the terms on the right hand side of Eq. (3) individually and together (filled symbols). The pressure term is always negative and tends to a constant value beyond about 50 h downstream of the manipulator, reflecting again the fact that three is no net drag reduction. The contribution from the integral on the right hand side is positive as mentioned earlier, but again tends to zero beyond about 50 h downstream of the manipulators. Two values for contribution from the manipulator drag are indicated in the figure: one assuming laminar flow on the blades, and another estimated from the careful direct measurements of device drag by Govindaraju and Chambers (1987). Beyond 50 h downstream of the manipulators, the right hand side of Eq. (3) is less than the manipulator drag, indicating that reduction in wall friction does give a relief. This relief amounts to 9–19% of the manipulator drag, depending on which of the two values for the latter is adopted.

It will be seen that the sum of terms III and IV in Eq. (3), as shown in Fig. 14, is not monotonic in x, suggesting that the contribution from term I is not either, i.e. that τ_{wm} is not always less than τ_w. We must remember however that Eq. (3) may not be applicable very near the manipulators due to possible normal pressure gradients across the channel in the wake.

The trend of variation of the various terms is similar in all the other cases as well. It is found that term III far downstream is always less than the laminar-flow drag of the manipulators, indicating a definite reduction in the channel wall friction drag in all cases. However, the pressure drop between any two stations is in all cases more than that in the free channel, demonstrating that there is no net drag reduction over any section of the channel.

4 Conclusions

It has been conclusively demonstrated that for all the manipulator configurations that have been studied here there is (but not surprisingly) a reduction in wall stress in the channel, but this reduction is too small to compensate for the manipulator drag even if the flow on the manipulator blades were to be completely laminar. It has recently been suggested (Pollard et al. 1990) that the manipulator configurations optimal for pipe flow may be somewhat different from those for boundary layers. Whether this is true for channels as well remains a matter for further investigation, but the rather low "relief" obtained in the present studies from wall stress reduction by manipulation does not offer much hope for achieving overall drag reduction unless the drag of the manipulator can itself be significantly reduced.

References

Acharya, M.; Escudier, M. P. 1983: Measurements of the wall shear stress in boundary layer flows. Proc. 4th Symp. Turbulent Shear Flows, pp. 277–286. Berlin Heidelberg New York: Springer

Anders, J. B.; Watson, R. D. 1985: Airfoil large eddy breakup devices for turbulent drag reduction. AIAA Paper 85-0520

Bertelrud, A.; Truong, T. V.; Avellan, F. 1982: Drag reduction in turbulent boundary layers using ribbons. AIAA Paper 82-1370

Bushnell, D. M. 1983: Turbulent drag reduction for external flows. AIAA Paper 83-0227

Corke, T. C.; Nagib, H. M.; Guezennec, Y. G. 1979: Modifications in drag of turbulent boundary layers resulting from manipulation of large scale structure. In Viscous flow drag reduction, Prog. Astro. Aero. 72, 128–143

Coustols, E.; Cousteix, J. 1986: Reduction of turbulent skin friction: Turbulence Moderators. 22nd AAAF Colloquium on Applied Aerodynamics, Lille, France, November 1985

Dean, R. D. 1978: Reynolds number dependence of skin friction and other bulk flow variables in two-dimensional rectangular duct flow. J. Fluids Eng. 100, 215–223

Govindaraju, S. P.; Chambers, F. W. 1987: Direct measurements of drag of ribbon-type manipulators in a turbulent boundary layer. AIAA J. 25, 388–394

Hefner, J. N.; Weinstein, L. M.; Bushnell, D. M. 1980: Large eddy breakup scheme for turbulent viscous drag reduction. Prog. Astro. Aero. 72, 110–127

Hefner, J. N.; Anders, J. B.; Bushnell, D. M. 1983: Alteration of outer flow structures for turbulent drag reduction. AIAA Paper 83-0293

Luchik, T. S.; Tiederman, W. G. 1987: Timescale and structure of ejections and bursts in turbulent channel flows. J. Fluid Mech. 174, 529–552

Mumford, J. C.; Savill, A. M. 1988: Manipulation of turbulent boundary layers by outer-layer devices. Skin friction and flow visualization results. J. Fluid Mech. 191, 389–418

Nagib, H. M. 1983: A new view on origin, role and manipulation of large scales in turbulent boundary layers. NASA-CR-165861
Narasimha, R.; Sreenivasan, K. R. 1985: The control of turbulent boundary layer flows. AIAA Paper 85-0519
Narasimha, R.; Sreenivasan, K. R. 1988: Flat plate drag reduction by turbulence manipulation. Sadhana 12, 15–30
Plesniak, M. W.; Nagib, H. M. 1985: Net drag reduction in turbulent boundary layers resulting from optimized manipulations. AIAA Paper 85-0518
Poddar, K.; Van Atta, C. W. 1985: Turbulent boundary layer drag reduction on an axisymmetric body using LEBU manipulators. Proc. 5th Symposium on Turbulent Shear Flows, Cornell University, Ithaca
Poll, D. I. A.; Watson, R. D. 1984: On the relaxation of a turbulent boundary layer after an encounter with a forward facing step. In: Improvement of aerodynamic performance through boundary layer control and high lift system, AGARD Conf. Proc. 365, 18.1-10
Pollard, A.; Savill, A. M.; Thomann, H. 1989: Turbulence pipe flow manipulation. J. Appl. Sci. Res. 46, 281–290
Pollard, A.; Thomann, H.; Savill, A. M. 1990: Manipulation and modelling of turbulent pipe flow. Proc. 4th European Drag Reduction Meeting, Lausanne; July 1989. To be published by Kluwer Academic (Editor: E. Coustols)
Prabhu, A.; Vasudevan, B.; Kailas Nath, P.; Kulkarni, R. S.; Narasimha, R. 1987: Blade manipulators in channel flows. In: Proc. IUTAM Symp. Turbulence Management & Relaminarization, Bangalore, pp 97–108. Berlin Heidelberg New York: Springer
Sahlin, A.; Johansson, A. V.; Alfredsson, P. H. 1988: The possibility of drag reduction by outer layer manipulators in turbulent boundary layers. Phys. Fluids 31, 2814–2820
Takagi, S. 1983a: The structure of turbulent boundary layer controlled by the plates. Proc. 15th Turbulence Symp., Tokyo
Takagi, S. 1983b: On the mechanism of drag reduction in a turbulent boundary layer using a thin plate. Proc. 2nd Asian Congress Fluid Mech, p. 292. Beijing, China: Sciences Press
Truong, T. V.; Bertelrud, A.; Veure, M. 1984: Boundary layer development of transverse ribbons. Abstracts, EUROMECH 181
Wilkinson, S. P.; Anders, J. B.; Lazos, B. S.; Bushnell, D. M. 1987: Turbulent drag research at NASA Langley – Progress and Plans. Presented at the Conference on "Turbulent drag reduction by passive means". Royal Aeronautical Society, London
Yajnik, K. S.; Acharya, M. 1987: Non-equilibrium effects in a turbulent boundary layer due to the destruction of large eddies. In: Structure and mechanisms of turbulence. Lecture Notes in Physics, 76, 249–260. New York: Springer

Received March 19, 1991

Technical notes

A simple lens-like method of determining small light ray deflections

H. Scheitle * and **S. Wagner**

Institut für Luftfahrttechnik und Leichtbau, Universität der Bundeswehr München, Werner-Heisenberg-Weg 39, D-8014 Neubiberg, FRG

List of symbols

d	lens thickness
f	focal distance
r	lens radius

Introduction

In various optical applications it is expedient to produce definite light deflections, e.g. for the calibration of the optical system. Schlieren and shadow methods take advantage of small light deflections to visualize flow fields. Suitable light deflections can be simulated by lenses as explained by Schardin (1941). There, a lens of some hundred meters focal length is used. The small curvature together with the high optical precision required lead to high production costs.

In the four colour line grid schlieren system described by Scheitle and Wagner (1990) a lens-like object, which is simple to manufacture, is used to adjust the knife edges. The same principle can be used to intensify the optical effect of small light deflections.

2 Design of a simple lens with large focal distance

The principle of the "lens" described here is to use a slightly bent parallel glass plate of small thickness. Depending on the bending radius and the thickness a light deflection results due to the slightly different incidence angles where a ray enters and exists the plate (Fig. 1). The lens can be designed to meet the requirement of the optical system. For small light deflections of a spherical lens the plot in Fig. 2 gives the dependence of the focal distance on radius and thickness of the glass plate for a refractive index of 1.5.

3 Application for small optical effects

In flow visualization small optical effects require a very sensitive apparatus, e.g. at supersonic expansion flow or in boundary layers. In these cases the lens decribed before can

* Present address: Motoren- und Turbinen-Union München GmbH, D-8000 München 50, FRG